Visual Neuroscience (2003), **20**, 363–372. Printed in the USA.

DOI: 10.1017/S0952523803204028

Temporal modulation sensitivity of tree shrew retinal ganglion cells

HAIDONG D. LU[1,*] AND HEYWOOD M. PETRY[1,2]

[1]Department of Psychological and Brain Sciences, University of Louisville, Louisville
[2]Department of Opthalmology and Visual Sciences, University of Louisville, Louisville

(RECEIVED July 1, 2002; ACCEPTED June 20, 2003)

Abstract

Tree shrews (*Tupaia belangeri*) are small diurnal mammals capable of quick and agile navigation. Electroretinographic and behavioral studies have indicated that tree shrews possess very good temporal vision, but the neuronal mechanisms underlying that temporal vision are not well understood. We used single-unit extracellular recording techniques to characterize the temporal response properties of individual retinal ganglion cell axons recorded from the optic tract. A prominent characteristic of most cells was their sustained or transient nature in responding to the flashing spot. Temporal modulation sensitivity functions were obtained using a Gaussian spot that was temporally modulated at different frequencies (2–60 Hz). Sustained cells respond linearly to contrast. They showed an average peak frequency of 6.9 Hz, a high-frequency cutoff at 31.3 Hz, and low-pass filtering. Transient cells showed nonlinear response to contrast. They had a peak frequency of 19.3 Hz, a high-frequency cutoff at about 47.6 Hz, band-pass filtering, and higher overall sensitivity than sustained cells. The responses of transient cells also showed a phase advance of about 88 deg whereas the phase advance for sustained cells was about 43 deg. Comparison with behavioral temporal modulation sensitivity results suggested that transient retinal ganglion cells may underlie detection for a wide range of temporal frequencies, with sustained ganglion cells possibly mediating detection below 4 Hz. These data suggest that two well-separated temporal channels exist at the retinal ganglion cell level in the tree shrew retina, with the transient channel playing a major role in temporal vision.

Keywords: Optic tract, Temporal vision, Temporal modulation sensitivity function, Transient cells, Sustained cells

Introduction

Tree shrews (*Tupaia belangeri*) are diurnal mammals closely related to primates (Butler, 1972; Luckett, 1980). Their cone-dominant retina contains two types of cones: long-wave-sensitive (LWS) cones and short-wave-sensitive (SWS) cones, and only ~5% rods (Müller & Peichl, 1989). Tree shrews, squirrels, and simian primates are the only mammalian groups with established cone-dominant retinas. It has been conjectured that cone-dominant retinas might be an adaptation for motion detection (Ahnelt & Kolb, 2000). The fast and agile movements of tree shrews in an arboreal environment indicate that they possess well-developed temporal vision. Behavioral (Schafer, 1969) and electroretinographic (ERG) studies (Tigges et al., 1967) have revealed a critical flicker frequency (CFF) of 75 Hz or more which is higher than the human CFF (i.e. ~50–60 Hz; de Lange, 1954; Kelly & Park, 1972). Whereas the CFF indicates the high-contrast temporal resolution of the visual system, temporal modulation sensitivity functions (tMSFs) provide a more complete description of the temporal properties of the visual system over a wide range of frequencies (de Lange, 1954, 1957; Kelly & Park, 1972). Temporal MSFs measured behaviorally in tree shrews revealed a peak sensitivity at about 15 Hz, a low-frequency roll-off, and a high-frequency cutoff beyond 50 Hz (Callahan & Petry, 2000). Thus, both CFF and tMSF results support the hypothesis that the properties of the tree shrew visual system facilitate high-frequency temporal information processing.

In most mammalian visual systems, different types of neurons usually have different temporal response characteristics, and likely play different roles in temporal information processing. In general, these neurons respond in either a sustained or a transient fashion to a change in visual stimulation. Sustained-type neurons respond continuously following the onset or offset of light with a very slow rate of adaptation. Transient-type neurons, on the other hand, respond primarily to the onset and/or offset of the light. Sustained-type and transient-type neurons have been found in many different species and at different levels of visual processing (Werblin & Dowling, 1969; Cleland et al., 1971; Schiller et al., 1976; Movshon et al., 1978; Kremers et al., 1991; Humphrey & Saul, 1993; Hawken et al., 1996). In the cat, it has been shown that morphologically different retinal ganglion cells (RGCs) differ in both their

Address correspondence and reprint requests to: Heywood M. Petry, Department of Psychological and Brain Sciences, Life Sciences Building, Room 317, University of Louisville, Louisville, KY 40292, USA. E-mail: woody.petry@louisville.edu

*Present address: Department of Psychology, Vanderbilt University, 111 21st Avenue South, Nashville, TN 37203, USA.

sustained/transient properties and in their linearity of spatial summation. Sustained responses are usually found in X-cells, which show linear spatial summation, while transient response are characteristic of Y-cells, which exhibit nonlinear spatial summation (Enroth-Cugell & Robson, 1966; Cleland et al., 1971). There are also differences in the temporal properties of cat X- and Y-RGCs (e.g. onset latency, amplitude sensitivity, temporal resolution, phase advance; Shapley & Victor, 1978; Victor & Shapley, 1979; Lennie, 1980; Frishman et al., 1987). At the level of the lateral geniculate nucleus (LGN), cat X- and Y-cells have been subdivided into lagged and nonlagged types based on their temporal response properties (Mastronarde, 1987*a*,*b*; Saul & Humphrey, 1990; Mastronarde et al., 1991). In short, the temporal tuning functions of lagged X- and Y-cells are shifted toward lower frequencies compared to their nonlagged counterparts (Saul & Humphrey, 1990, 1992; Wolfe & Palmer, 1998). It is still unresolved whether lagged and nonlagged responses represent different classes of neurons (Humphrey & Saul, 1992; Hartveit & Heggelund, 1993) or simply two response modes of the same cells which receive different influences from the brain stem (Uhlrich et al. 1990; Lu et al., 1995).

In primates, P- (color-opponent) and M- (spectrally broad band) cells also show differences in their temporal properties. The P-cells usually have sustained (tonic) responses; their sensitivity to luminance contrast is lower and they prefer lower temporal frequencies (i.e. a peak frequency of about 10 Hz, Derrington & Lennie, 1984). The M-cells, in contrast, usually have a transient (phasic) type of response; have higher sensitivity to luminance contrast, and prefer higher temporal frequencies (i.e. a peak frequency of about 20 Hz, Derrington & Lennie, 1984). Compared to the relatively linear response of P-cells, M-cells show more nonlinear features. For example, when stimulus contrast is increased, their contrast gain decreases (i.e. displaying a contrast gain control mechanism), their peak sensitivity shifts to higher frequencies, and their response phase advances (Benardete et al., 1992).

In the tree shrew, the neuronal mechanisms underlying temporal sensitivity have not yet been investigated, although neurons with sustained and transient response properties have been found in the optic tract (van Dongen et al., 1976; Thijssen et al., 1976; ter Laak & Thijssen, 1978), in the LGN (Sherman et al., 1975; Holdefer & Norton, 1995), and in the visual cortex (Norton et al., 1985; Lu & Petry, 2001). This finding of a sustained/transient dichotomy suggests the presence of different temporal processing channels in the tree shrew visual system. In the tree shrew retina, three major types of RGCs have been classified morphologically based on axon diameter, soma area, and dendritic field (DeBruyn, 1983; Drenhaus et al., 1997). Electrophysiological recordings made in the optic tract (van Dongen et al., 1976) revealed that cells with sustained and transient response properties each comprise about one-third of the RGCs. The other third exhibited response properties ascribed to W-like cells. Many important properties of tree shrew RGCs (e.g. temporal and spatial frequency response properties, temporal and spatial linearity, etc.) have not been examined. The present study used single-unit recording techniques to explore the temporal properties of tree shrew RGCs focusing on the measurement of temporal modulation sensitivity functions (tMSFs).

Methods

Data was collected from 11 tree shrews (*Tupaia belangeri*) with body weight 155–223 g. All were colony reared and were sexually mature adults ($\geq$4 months of age) at the time of recording. The care and treatment of all animals was in strict accordance with NIH and institutional IACUC guidelines.

Standard single-unit extracellular recording techniques were used. Tree shrews were initially anesthetized with halothane (4–5%) followed by ketamine (15–25 mg, i.m.). Atropine (0.03 mg) was applied to reduce salivation and bronchial secretion. After the cannulation of the trachea, tree shrews were moved to a stereotaxic apparatus where gas anesthesia [nitrous oxide (70%)/oxygen (30%) with supplemental halothane (0.2–1%)] was initiated, then maintained. Artificial respiration was begun after a muscle relaxant (gallamine triethiodide, 20 mg/kg/h) was applied (i.m.). Local anesthesia (Lidocaine 1%) was applied during the tracheal and craniotomy surgeries. In addition, a topical anesthetic (Proparacaine HCl 0.5%) was applied to the cornea. Pupils were dilated with atropine sulphate (1%) and plano contact lenses were used to prevent dehydration of the corneas. The physiological status of the animal was continuously monitored by recording its electrocardiogram, body temperature, and expired end-tidal CO_2 (which was maintained at approximately 5%).

Because of the relatively small eyes of the tree shrew, RGC responses were recorded from their axons in the optic tract. Glass-coated and Parylene-C-coated tungsten electrodes with 1–10 μm tip exposure and 3–5 MΩ impedance were used. A craniotomy was made above the optic tract, and mineral oil was applied to the exposed brain surface. The electrode was lowered into the optic tract through the brain with a hydraulic microdrive. When a cell was found, its receptive-field (RF) location was first determined by using a hand-held reverse ophthalmoscope (Keeler Instruments Inc), then detailed RF properties were tested with visual stimuli delivered by a computer-controlled CRT monitor. A spatial-temporal map of the RF (Bullier & Norton, 1979) was obtained by stepping a bar of light toward, through, and away from the RF both vertically and horizontally, which usually revealed a clear center-surround organization of the RF. Other visual stimuli (e.g. a light spot, an annulus with increasing/decreasing size, a small light dot sweeping through a rectangular area which cover the RF) also helped to determine the RF shape and center/surround organization. The amplified cell response was windowed, digitized, plotted on-line, and recorded by another computer at 500-Hz sampling frequency. The neuronal signal was also audio-monitored and visualized on an oscilloscope.

The temporal properties of individual cells were characterized using two types of stimuli: a flashing spot stimulus and a Gaussian spot modulated sinusoidally over time at different temporal frequencies. The flashing spot stimulus consisted of a white spot on a dark background that was flashed at 1-Hz frequency (500 ms bright and 500 ms dark) for 20 s. The spot size was adjusted to cover the cell's RF center. Response histograms were constructed from 20 presentations of the stimulus. Spontaneous activity was recorded for 15 s both before and after the stimulus presentation. The degree of transiency of a neuron's response was determined by its transient–sustained index (*TSI*). This measure was calculated from the histograms according to the following formula:

$$TSI = 100 - 100 \times (R_s - M)/(R_t - M),$$

where R_s is the average response from 200 ms to 400 ms after visual stimulus onset (sustained component); R_t is the average response during the first 200 ms of stimulation (transient component), and M is the spontaneous activity. The same calculation was used for OFF-cells except that responses were measured from the

OFF portion of the response. Cells with a larger transient response will have a higher *TSI*.*

For the sine-wave temporal modulation test, the receptive-field center was stimulated by a luminance-modulated edgeless circular patch (Gaussian spot), in which the luminance was sinusoidally modulated above or below the background luminance. The temporal modulation depth or "contrast" of the stimulus was calculated as $100 \times (L_{\max} - L_{\min})/(L_{\max} + L_{\min})$ (Michelson contrast), in which $L_{\max}$ represents the maximum luminance and $L_{\min}$ the minimum luminance. For each cell, temporal sensitivity was tested at seven different frequencies (2, 4, 10, 15, 20, 30, and 60 Hz). At each frequency, the contrast was varied incrementally then decrementally (0% → 100% → 0%) in seven steps: 0%, 16%, 33%, 50%, 67%, 83%, and 100%. Each step was 3.5 s in duration and separated by 0.5 s of background luminance. The background luminance of the screen was kept at 34 cd/m^2 [which permitted direct comparison with the previous behavioral study: Callahan & Petry (2000)]. All cells were evaluated for their ON–OFF and sustained/transient properties. Complete tMSFs were obtained from about 50% of the cells. Due to the length of the test (*ca.* 30 min), some cells were not held long enough for completion of all the tests. To assess potential drift in the cells' responsivity during the 30-min testing period, the initial stimulus condition was repeated at the end of the series of tests. If the cell's response had changed, the data was not used. The temporal resolution of a subset of cells was assessed by listening to the cell's response through the audio monitor while varying the temporal frequency of a light-emitting diode (LED) stimulus driven by a function generator (Wavetek, Inc., San Diego, CA).

In off-line data analysis, the spike train at each contrast level was first averaged, and then analyzed into Fourier components at each of the stimulus frequencies. The first harmonic component was used as the response index. The two measurements at the same contrast level obtained during the rising and falling portions of stimulus presentation were averaged and plotted to construct a "Response–Contrast Curve." These response–contrast curves then were fitted by the radiance-response function (Naka & Rushton, 1966) in the form of

$$R_{(C)} = R_0 + R_m C/(C + b),$$

in which $R_{(C)}$ is the response and C is the contrast, and R_0, R_m, and b are fitting parameters. Contrast gain (the initial slope of the *R–C* curve) was estimated from the ratio of R_m/b in units of firing rate per unit contrast (impulses/s/%) (Lee et al., 1994; Yeh et al., 1995). Temporal MSFs were fitted to a double exponential function (Wilson, 1978; Dobkins et al., 1999) using SigmaPlot software (SPSS Inc., Chicago, IL). The function has the following expression:

$$a(\omega b)^d \exp(-c\omega b),$$

where ω is the temporal frequency, and a, b, c, d are fitting parameters. Peak sensitivity (i.e. maximum contrast gain), peak frequency (i.e. the temporal frequency yield peak sensitivity), and high-cutoff and low-cutoff frequencies (i.e. defined as that frequency at which the response dropped to half-maximum amplitude) were determined from the fitted functions. For cells with low-pass MSFs, no low-cutoff frequency was determined.

*This index is a combination of the Phasic-Tonic-Index (*PTI*, Norton & Casagrande, 1982; Holdefer & Norton, 1995), and the Transient-Index (*TI*, Schiller & Malpeli, 1977, 1978).

Results

A total of 65 retinal ganglion cell responses were recorded from the optic tracts of 11 animals. Most cells (90%) had concentric, center-surround RFs located within the central 40 deg of the visual field. Similar to previous findings (van Dongen et al., 1976), the majority of cells showed either a sustained or a transient response to the flashing spot. Sustained and transient cells were found at all eccentricities and no significant differences were found in the mean eccentricity values of these two groups of cells. All RF centers could be classified as ON (50/65), OFF (11/65), or ON–OFF (4/65) types. Only ON and OFF cells ($n = 61$) were studied here.

Sustained/transient properties

Sustained cells usually maintained a response rate of about 50% of maximum response after the initial burst (see Fig. 1), whereas transient cells generally responded only briefly to the onset or offset of the flashing spot. Their response usually was limited to the initial 100–150 ms period (see Fig. 1). To quantify the sustained/transient properties, the transient-sustained index (*TSI*) of each cell (see Methods) was used. As shown in Fig. 2, the distribution of *TSI* values was bimodal. The *TSI* distribution was fitted with two Gaussian distributions with least-square regression methods ($R^2 = 0.88$). These two fitting curves have peaks (i.e. means) at $TSI = 33$ and $TSI = 93$, respectively, and cross at $TSI = 68$. By this criterion, 38 cells were classified as sustained cells ($TSI < 68$) and 23 cells were classified as transient cells ($TSI \geq 68$). The ratio of sustained cells to transient cells was approximately 1.7:1. The sustained group had a mean *TSI* of 31.9 ± 16.3 (mean ± S.D.), whereas the transient group had a mean *TSI* of 92.2 ± 13.3. A *TSI* value higher than 100 occurs when the sustained response is lower than the maintained response (i.e. presence of inhibition). A negative *TSI* occurs when the sustained response is higher than the transient response. The onset latency (i.e. the time from stimulus onset to the point at which the cell's response exceeded its spontaneous level) was also measured for each response histogram. The onset latency for sustained cells was 3.1 ms longer than that for transient cells (34.3 ± 4.2 ms *vs*. 31.2 ± 3.5 ms, *t*-test, $P < 0.01$).

Temporal modulation sensitivity function (tMSF)

Of the 61 cells recorded, tMSFs were obtained from 31 cells (18 sustained cells and 13 transient cells). For every temporal frequency, the phase of the first harmonic response was measured at each contrast level tested. The cells' responses to different stimulus frequencies usually were characterized by different phase shifts, although within a given frequency the response phase did not vary systematically with contrast. This may have been due to the fairly large stimulus contrast steps used (i.e. 0, 16.7%, 33.3%. . .) and because gain control mechanisms have been shown to affect response phase primarily at low contrasts (e.g. Victor, 1987; Yeh et al., 1995). Due to the lack of systematic variation across contrast level, a response phase value was obtained for each frequency by averaging across all contrast levels tested. This analysis revealed that this phase measurement decreased proportionally as temporal frequency increased. In a phase-frequency plot, the slope of the linear regression line represents the response latency (Lee et al.

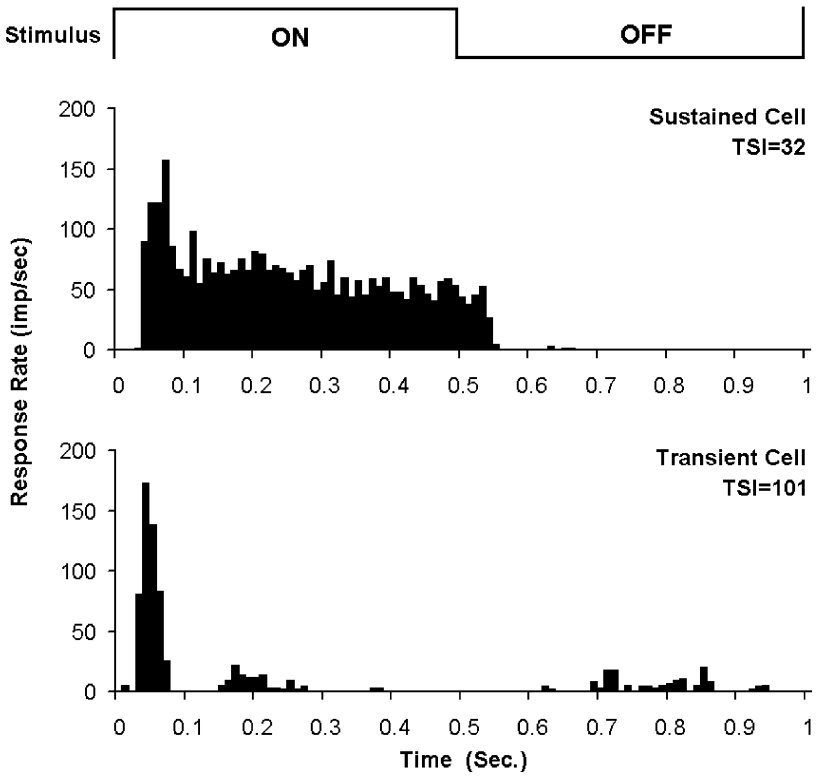

Fig. 1. The response histograms of one sustained ON-cell (*TSI* = 32) and one transient ON-cell (*TSI* = 101) to a white spot flashed at 1 Hz on a black background (contrast near 100%) covering the RF center. The time course of the stimulus(0.5 s ON and 0.5 s OFF) is shown on the top. Histograms were constructed from 20 presentations of the stimulus. Bin width: 10 ms; *TSI*: transient-sustained index.

1981, Frishman et al., 1987). Our results showed that the phase difference caused by response latency changed linearly with the stimulus frequency. The phase response may also be characterized by the *y* intercept of the phase-frequency plot (i.e. the interception of the regression line with the phase axis). This value also may reflect an intrinsic property of the cell, and has been described as the cell's absolute phase (Saul & Humphrey, 1990), or its constant phase shift (Lankheet et al., 1989). In our data, a significant difference was observed between the absolute phases of sustained cells and transient cells. Sustained cells were more homogenous in this feature, showing a phase advance of 43 deg ± 10 deg in contrast to 88 deg ± 28 deg phase advance for transient cells (*t*-test, $P < 0.001$). Three cells in the transient group (average *TSI* = 85) had unusually low phase advances (39–54 deg), which suggests that there might be subgroups of transient cells. Without these three cells, the other ten cells had mean phase advance of 101 deg ± 16.4 deg. The response of two representative cells to 2-Hz modulation is shown in Fig. 3. These data indicate that transient

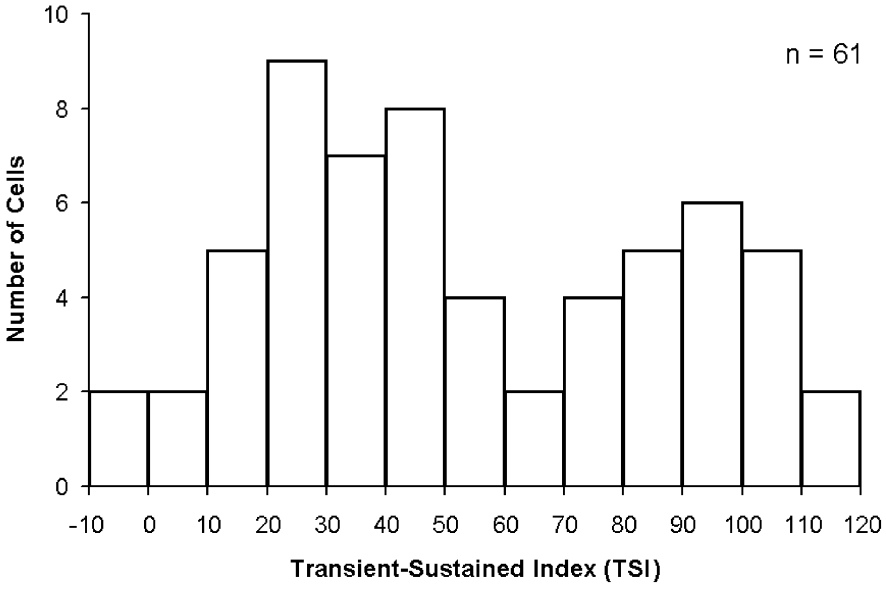

Fig. 2. Distribution of the transient-sustained index (*TSI*) values of 61 retinal ganglion cells recorded from the optic tract. *TSI* values were measured from the response histograms (as shown in Fig. 1). A higher *TSI* value indicates a more transient response. Details of the calculation of *TSI* are described in Methods.

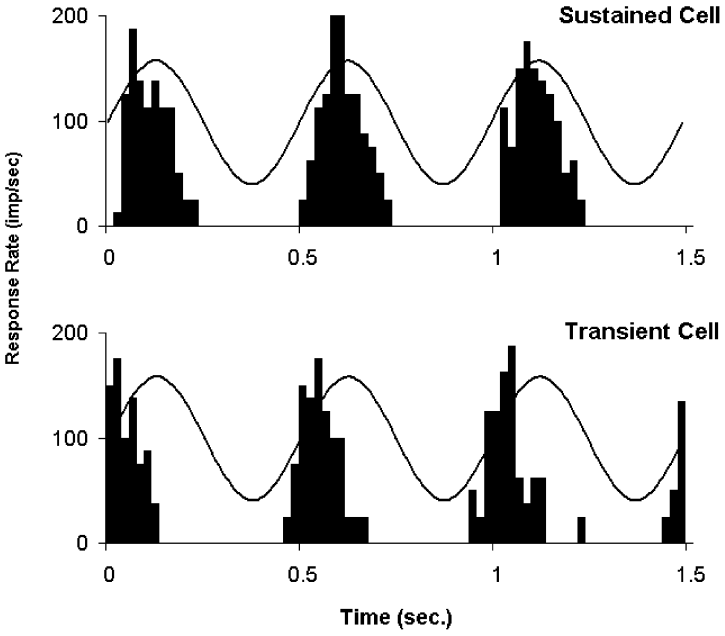

Fig. 3. Response of two representative cells to 2-Hz sine-wave temporal modulation. The smooth curves represent the sine-wave modulated stimulus (a Gaussian spot modulated at a contrast level of 67%). The sustained cell's response shows a phase advance of 29 deg leading the stimulus. The transient cell's phase advance is 80 deg. Each response is averaged from two 3-cycle presentations. Bin width: 20 ms.

cells were responding to luminance changes rather than to luminance level. It is interesting that although sustained cells mainly responded when the stimulus luminance was higher than the background level, they also showed about a 43-deg phase advance.

Fig. 4 shows the *R–C* curves of one sustained cell and one transient cell. For clarity, only four of seven temporal frequencies are shown for each cell. Most sustained cells had *R–C* curves like the sustained cell shown in Fig. 4 (left): the response increased linearly with the contrast, a lower contrast gain was observed (i.e. shallow slopes of *R–C* curves), and little saturation was displayed (some cells saturated at a relatively high contrast level of 40–80%). In contrast, the *R–C* curves of most transient cells had the pattern of the transient cell shown in Fig. 4 (right), showing a high contrast gain and saturation at contrast levels between 20–60%. That different frequencies can be saturated at different response levels (e.g. 4 Hz saturated at 40 impulses/s and 30 Hz saturated at 80–100 impulses/s) indicates that saturation is not simply limited by the maximum firing rate of the cell, but likely results from contrast gain control mechanisms. Contrast gain also depended on the mean luminance level, since saturation decreased with mean luminance level (data not shown).

Temporal frequency sensitivity (measured as contrast gain) was fitted with a double exponential function. Fig. 5 shows the tMSFs of the cells shown in Fig. 4. The sustained cell had a low-pass feature over the frequency range of measurement and its response dropped quickly beyond 20 Hz. In contrast, the transient cell was band-pass and had a much higher overall sensitivity. (Note the difference in scales.) These features were characteristics of sustained and transient cell groups in general, although several transient cells did show a shallow drop at the low frequency end. Sustained cells had a mean peak frequency of 6.9 ± 3.8 Hz and a high cutoff at 31.3 ± 19.0 Hz. Both values are lower than those of

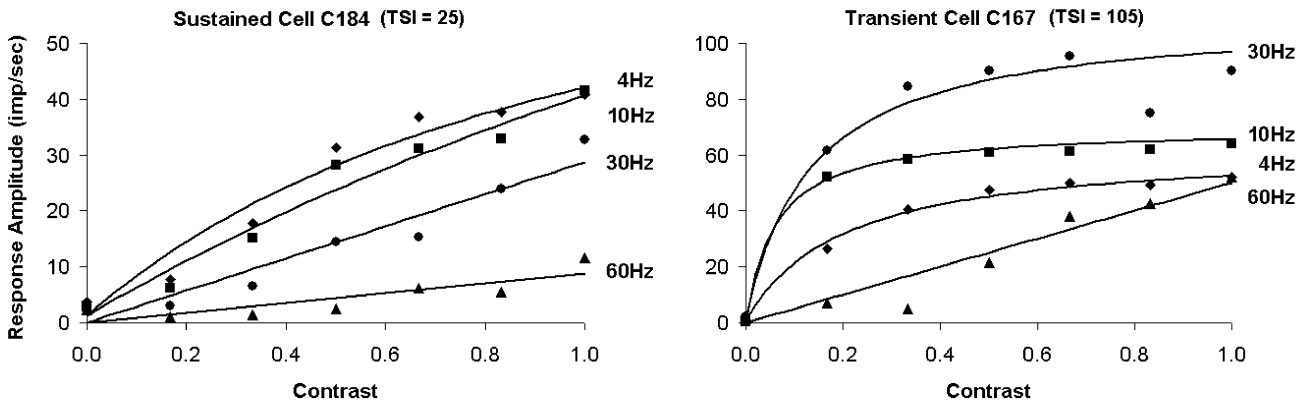

Fig. 4. Response-contrast (*R–C*) curves of two representative cells. The response of the sustained cell is linear and increases with stimulus contrast without appreciable saturation. The response of transient cell begins to saturate at about 20% contrast for most temporal modulations except for 60 Hz. Stimulus frequencies are indicated for each curve. Note that the two plots have different scales. (Response amplitude: first-harmonic amplitudes from Fourier analysis.)

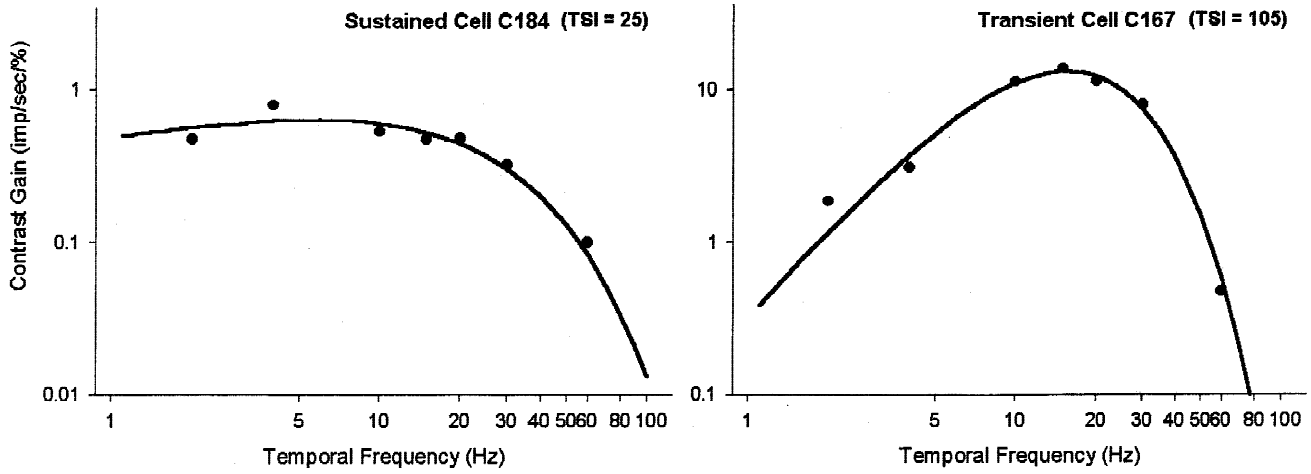

Fig. 5. Temporal modulation sensitivity functions (tMSFs) of the sustained and transient cells shown in Fig. 4. Sensitivity was measured as contrast gain at low contrast level (i.e. the initial slope of the *R–C* curves) and was fitted with a double exponential function. Note that the two plots have different sensitivity scales.

transient cells (peak: 19.3 ± 8.6 Hz, *t*-test, $P < 0.001$, high cutoff: 47.6 ± 26.7 Hz, $P < 0.05$). In addition, the mean peak sensitivity of transient cells (4.2 impulses/s/%) is about three times that of sustained cells (1.4 impulses/s/%, *t*-test, $P < 0.01$). The temporal resolution (the highest frequency at which a noticeable visual response could be heard) was also lower for sustained cells than transient cells, although this was not tested systematically (see Methods). For the subset of cells tested using a function-generator-driven LED, some transient cells showed the capability of following frequencies up to 80–100 Hz while sustained cells stopped following at 50–80 Hz.

Fig. 6 shows the tMSFs of 18 sustained cells and 13 transient cells. For clarity, the tMSF curves were shifted vertically according to cells' *TSI* values. Temporal MSFs were first plotted in log–log units then scaled by a factor of 20 to be comparable with the *TSI* unit. Each curve was then shifted vertically to align the *y* value of its peak with its *TSI* value (right axis). Sustained cells ($TSI < 68$) have flatter curves and peak at 2–17 Hz (mean = 6.9 Hz). Transient cells ($TSI \geq 68$) generally have inverted U-shaped curves with peaks ranging from 6 Hz to 37 Hz (mean = 19.3 Hz). Sustained cells show a general trend of an increasing high-frequency cutoff value with increasing degree of transiency (higher *TSI*). This trend is not obvious in the transient cell group.

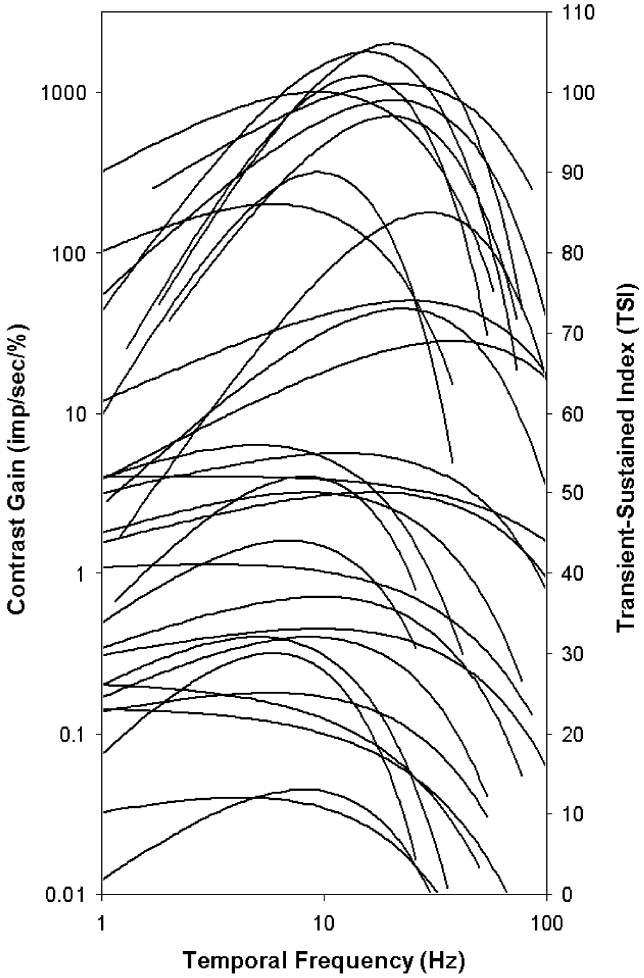

Fig. 6. Temporal modulation sensitivity functions (tMSFs) of 31 retinal ganglion cells (18 sustained cells and 13 transient cells). For clarity, each curve was vertically shifted to align the *Y* value of its peak with its *TSI* level. Most, but not all sustained cells (with $TSI < 68$) have a low-pass feature while most, but not all transient cells ($TSI \geq 68$) are band-pass and peak at higher frequencies.

Discussion

The temporal response patterns of visual neurons to a flashed stimulus vary enormously across species and systems (Kuffler, 1953; Cleland et al., 1971; Schiller et al., 1976; Movshon et al., 1978; Kremers et al., 1991; Humphrey & Saul, 1993; Hawken et al., 1996). However, a common feature is a separation into cells with brief transient responses or prolonged sustained responses. Recent studies showed that this kind of parallel processing of temporal information could begin at the first synapse in the visual system between cone photoreceptors and bipolar cells (DeVries, 2000; Awatramani & Slaughter, 2000). In this study, we showed that the temporal properties of sustained and transient ganglion cells in the tree shrew retina differ in many aspects, including onset latency, phase advance, peak frequency, bandwidth, sensitivity amplitude, and contrast gain. Sustained and transient cell types are

also evident in the tree shrew LGN and striate cortex (Sherman et al., 1975; Norton et al., 1985, Holdefer & Norton, 1995; Lu & Petry, 2001). This cellular emphasis on temporal characteristics of the stimulus is reflected in the visual abilities of the animal. Behavioral studies have shown that tree shrews have very good temporal vision (Schafer, 1969; Callahan & Petry, 2000), but relatively poor spatial contrast sensitivity (Petry et al.,1984).

To permit comparison of our results with the behavioral data, RGC sensitivity was estimated from averaged contrast gain by defining a threshold response of 10 impulses/s in the first harmonic response (i.e. a modulation of 20 impulses/s, see Lee et al., 1990). Fig. 7 shows the RGC sensitivity for transient and sustained cells. Each data set was fitted with a double exponential function and the curves shifted vertically to match with the peak of the behavioral tMSF. Since the temporal sensitivity of individual cells is often influenced by the retinal adaptation level, the contrast, and the spatial configuration of the stimulus being used, it is important to note that the cell data was collected under ambient light conditions (34 cd/m^2) identical to that used in the behavioral study. The RGC sensitivity estimates were obtained from the initial slope of fitted *R–C* curves. It is also relevant that our data represents sensitivity at low contrast levels, since it has been found that higher levels of contrast will shift peak sensitivity to a higher temporal frequency (Kremers et al., 1992; Sclar, 1987). Thus, the conditions under which we have estimated neuronal response (i.e. close to threshold detection) should be comparable to the psychophysical testing conditions.

The averaged transient tMSF shows good overlap with behaviorally obtained tree shrew tMSF data that were measured at five frequencies: 3.7, 7.3, 14.7, 29.3, and 46.9 Hz (Callahan & Petry, 2000). The behavioral and transient cell tMSFs have similar peak frequencies (at about 15–20 Hz) and similar shapes. These correspondences suggest that transient cells may underlie detection over a wide range of temporal frequencies. Compared with the behavioral data, the tMSF of the transient retinal ganglion cells shows a small shift towards higher frequencies, which may suggest a low-pass filtering at higher levels of temporal processing. Similar differences between higher and lower levels of temporal information processing have also been observed in cat (Sturr & Shansky, 1971) and monkey (Hawken et al., 1996). The absolute sensitivities of the sustained and transient cells reverse at about 4 Hz, so that the sustained cells are more sensitive. Since the lowest frequency tested in the behavioral experiments was 3.7 Hz, it is possible that sustained cells mediate motion detection at frequencies lower than 4 Hz.

The visual systems of the cat and the monkey have been studied extensively in the past and provide an interesting comparison. One striking difference is that whereas cat X- and Y-RGCs and LGN cells are well distinguished by their spatial properties (i.e. linear or nonlinear spatial summation, Enroth-Cugell & Robson, 1966; Hochstein & Shapley, 1976*a*,*b*), the spatial properties of sustained and transient cells in the tree shrew LGN and of P- and M-cells in monkey are more homogenous. For example, in the tree shrew dLGN, (data for tree shrew RGCs are lacking), 97% of neurons recorded in LGN layers 1, 2, 4, and 5 (which receive input from moderate-to-large RGCs, and project to layer IV of striate cortex, DeBruyn, 1983; Conley et al., 1984) showed linear spatial summation (Holdefer & Norton, 1995). Studies of monkey RGCs and LGN neurons have reported that P-cells and most M-cells are also linear in spatial summation (Kaplan & Shapley, 1982; Benardete & Kaplan, 1999). In the temporal domain, cat X- and Y-cells, like tree shrew RGCs, show differences in temporal response features, such as transient/sustained features, differences in onset latency, phase advance, etc. (Cleland et al., 1971; Hochstein & Shapley, 1976*a*, Frishman et al., 1987). The temporal sensitivity functions of cat X- and Y-RGCs tend to have similar peak amplitudes and peak frequencies (at *ca* 8–10 Hz) when they are tested at optimal spatial frequencies, but Y-cells display a higher temporal resolution (e.g. Shapley & Victor, 1978; Victor & Shapley, 1979; Lennie, 1980; Frishman et al., 1987). For stimuli presented at frequencies lower than the optimal spatial frequency for each cell, temporal tuning functions of both X-cells and Y-cells shift toward higher temporal frequencies, and tend to have a narrower bandwidth. Under these conditions, X-cells display higher peaks frequencies than Y-cells, which is indicative of their strong antagonistic surround (Frishman et al., 1987). X-cells also show contrast gain control mechanisms

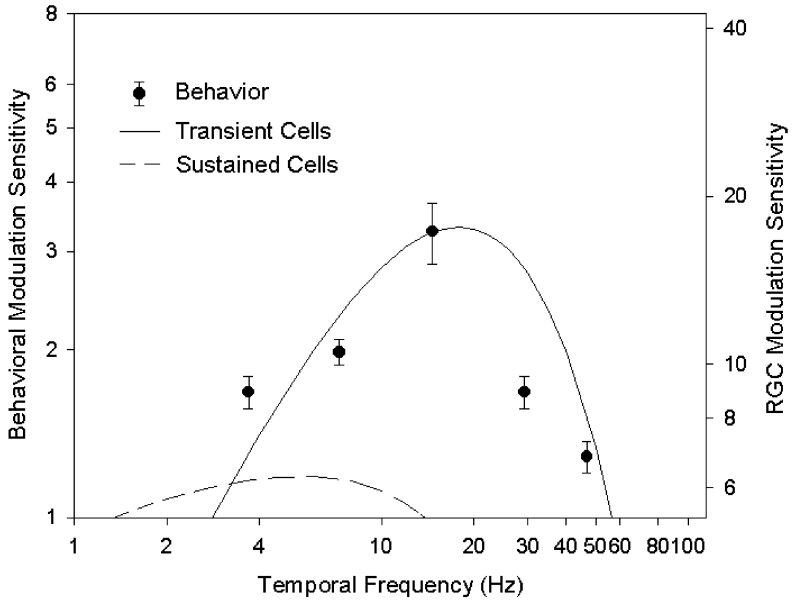

Fig. 7. Comparison of averaged temporal modulation sensitivity functions (tMSFs) for 18 sustained cells (dashed line) and 13 transient cells (solid line) with behaviorally obtained data (black dots, error bar: SEM) obtained at 3.7, 7.3, 14.7, 29.3, and 46.9 Hz (Callahan & Petry, 2000). The cellular sensitivity was estimated from averaged contrast gain by defining 10 impulses/s as the threshold response, fitting with double exponential functions, and then vertically shifting the function to match with the peak of the behavioral MSFs.

in responding to increasing contrast (Shapley & Victor, 1978, 1979). This is quite different from sustained cells in tree shrew (this study) and P-cells in monkey (Shapley & Perry, 1986; Benardete et al., 1992), where little, if any, evidence of contrast gain control mechanisms were seen. In a whole-cell patch-clamp study with sinusoidal current injections, it was shown that cat X- and Y-RGCs have equivalent intrinsic temporal properties (Robinson & Chalupa, 1997). These cells also have a common input from transient b1 bipolar cells, which defines the transient portion (initial burst) of the response and possibly underlies the similar peak frequencies of X- and Y-RGCs (Freed, 2000). The sustained portion of the response found in X-cells may reflect their b2/b3 bipolar inputs, which are minimal in Y-cells (Freed & Sterling, 1988; Freed, 2000). In the primate retina, M-cells are more transient than P-cells. They have larger phase advance and respond to higher temporal frequencies. When tested with luminance gratings, M-cells showed much higher contrast gain (8–10 times) than P-cells. (Kaplan & Shapley, 1986; Lee et al. 1989). However, most P-cells respond better to chromatic modulation. If calculated in terms of cone contrast, sensitivities of P-cells to chromatic modulation are more comparable to sensitivities of M-cells to achromatic modulation, differing only by a factor of 2–3 (Lee et al., 1989, 1993). This is similar to the ratio of 3 we found in the tree shrew, considering that both sustained and transient cells receive only LWS cone input (see discussion below). In responding to contrast, P-cells show a general linear response to increasing contrast. M-cells, however, exhibit strong nonlinearity in their response. Their contrast gain decreases when stimulus contrast increases, nevertheless, such contrast effect is more significant at low temporal frequencies than at higher temporal frequencies (Kaplan & Benardete, 2001). We found tree shrew sustained and transient RGCs to be similar to P- and M-cells in this feature. As shown in Fig. 4, sustained cells responded linearly to contrast while transient cells showed significant nonlinearity.

Any differences in the parallel processing of visual information by sustained and transient pathways will be amplified by differences in the relative numbers of transient and sustained RGCs. The ratio of transient cells to sustained cells (1:1.7) found in the present study is similar to the transient:sustained cell ratio of 1:1 found in prior electrophysiological recordings from the optic tract (van Dongen et al., 1976). Keeping in mind a likely electrode bias for the thick axons of large cells, there is rough agreement between these transient:sustained ratios and the ratios of the large- and mid-sized RGCs in the retina (DeBruyn, 1983). In a detailed morphological analysis of the tree shrew retina, DeBruyn found that the ratio of Type I RGCs (large cells analogous to cat alpha cells) to Type II RGCs (smaller cells analogous to cat beta cells) varied from 1:4.3 in the area centralis to 1:1 in the periphery. Using DeBruyn's estimate for the Type I population and their own measurements of axon diameter, Drenhaus et al. (1997) modeled the distribution of axons in the tree shrew optic nerve and described the ratio of large- to medium-sized axons as 1:2. The data from each of these electrophysiological and anatomical studies indicate a substantially higher percentage of transient/large RGCs in the tree shrew retina compared to other species. For example in the cat retina, the ratio of alpha cell (Y-cells) to beta cells (X-cells) is about 1:11 (see review by Troy & Shou, 2002). In fact, Peichl et al. (1987) reported that alpha RGCs never made up more than 1–4% of total RGCs across a variety of mammalian species including cat, ferret, mink, dog, chinchilla, and rabbit. In the macaque retina, the ratio of parasol cells (M-cells) to midget cells (P-cells) has been estimated at 1:8 (Perry et al., 1984; Watanabe & Rodieck, 1989; Silveira & Perry, 1991). In the tree shrew retina, the relatively higher proportion of transient cells, their enhanced temporal properties, and the broad range of frequencies to which they are sensitive supports an emphasis of the transient pathway in the tree shrew visual system. Like its highly cone-dominated photoreceptor population, an emphasis on processing of temporal information may reflect an adaptation to the tree shrew's life style and environmental niche (Langham, 1982; see also Ahnelt & Kolb, 2000). Tree shrews are fast moving, agile, and show proficiency in navigating arboreal environments, abilities that require well-developed temporal vision and motor system control. It is likely that the tree shrew's visual system has evolved in such a way that temporal information processing is emphasized, and that this emphasis begins at the earliest visual processing stages.

We also assessed the properties of each cell with regard to cone activation. Although the tree shrew retina has two types of cones (LWS and SWS cones; Petry & Hárosi, 1990), and behavioral studies show that tree shrews have dichromatic deutan-type color vision (Polson, 1968; Jacobs & Neitz, 1986; Petry & Kelly, 1991), none of our 65 sampled cells displayed clear color opponency. Color-opponent cells were also rare (1 of 96) in the only other published electrophysiological study of tree shrew optic tract fibers (van Dongen et al., 1976). It is possible that this lack of color cells may have been due to microelectrode sampling characteristics, which also may have led to the predominance of ON-cells in our data. Since ON- and OFF-cells are segregated into different LGN laminas, it is possible that ON- and OFF-optic tract fibers also tend to cluster together before reaching LGN. If the OFF-fibers were clustered toward the ventral portion of the optic tract, it is possible that they would have been missed by our recordings. To prevent damage to microelectrodes (the optic chiasm and rostral part of optic tract sit just dorsal to the tree shrew skull), our deepest recording depth was usually 10,000–11,000 μm measured from the brain surface.

In summary, the present study has extended knowledge of the temporal properties of sustained and transient parallel pathways in the mammalian retina. Results showed that the tMSFs of ganglion cells in these two groups differed from one another in a consistent manner. Compared to sustained cells, transient cells had an overall higher sensitivity, peaked at higher frequencies and better resembled the behavioral results. These properties make them best suited for conveying information about all but the lowest of temporal frequencies to higher levels of the visual system. Sustained cells displayed a low-pass tMSF and may play an important role in the detection of temporal frequencies below 4 Hz.

Acknowledgments

We thank Dr. Martha Bickford for her critical reading of this manuscript. This work was supported by a Sigma Xi Grant-in-Aid of Research, and by NSF-KY-EPSCoR (# OSR-9452895).

References

Ahnelt, P.K. & Kolb, H. (2000). The mammalian photoreceptor mosaic-adaptive design. *Progress in Retinal and Eye Research* **19**, 711–777.

Awatramani, G.B. & Slaughter, M.M. (2000). Origin of transient and sustained responses in ganglion cells of the retina. *Journal of Neuroscience* **20**, 7087–7095.

Benardete, E.A. & Kaplan, E. (1999). The dynamics of primate M retinal ganglion cells. *Visual Neuroscience* **16**, 355–368.

Benardete, E.A., Kaplan, E. & Knight, B.W. (1992). Contrast gain control in the primate retina: P cells are not X-like, some M cells are. *Visual Neuroscience* **8**, 483–486.

Bullier, J. & Norton, T.T. (1979). X and Y relay cells in the cat lateral geniculate nucleus: Quantitative analysis of receptive-field properties and classification. *Journal of Neurophysiology* **42**, 244–273.

Butler, P.M. (1972). The problem of insectivore classification. In *Studies in Vertebrate Evolution,* ed. Joysey, K.A. & Kemp, T.S., pp. 253–265. Edinburgh, UK: Oliver and Boyd.

Callahan, T.L. & Petry, H.M. (2000). Psychophysical measurement of temporal modulation sensitivity in the tree shrew (*Tupaia belangeri*). *Vision Research* **40**, 455–458.

Cleland, B.G., Dubin, M.W. & Levick, W.R. (1971). Sustained and transient neurons in the cat's retina and lateral geniculate nucleus. *Journal of Physiology* **217**, 473–496.

Conley, M., Fitzpatrick, D. & Diamond, I.T. (1984). The laminar organization of the lateral geniculate body and the striate cortex in tree shrew (*Tupaia glis*). *Journal of Neuroscience* **4**, 171–197.

DeBruyn, E.J. (1983). *The organization and central terminations of retinal ganglion cells in the tree shrew* (*Tupaia glis*). Doctoral Dissertation, Vanderbilt University, Nashville, TN.

de Lange, H. (1954). Relationship between critical flicker frequency and a set of low-frequency characteristics of the eye. *Journal of the Optical Society of America, A—Optics Image Science and Vision* **44**, 380–389.

de Lange, H. (1957). *Attenuation characteristics and phase-shift characteristics of the human fovea-cortex system in relation to flicker-fusion phenomena*. Doctoral Dissertation, Technische Hogeschool, Delft.

Derrington, A.M. & Lennie, P. (1984). Spatial and temporal contrast sensitivities of neurons in lateral geniculate nucleus of macaque. *Journal of Physiology* **357**, 219–240.

DeVries, S. (2000). Bipolar cells use kainate and AMPA receptors to filter visual information into separate channels. *Neuron* **28**, 847–856.

Dobkins, K.R., Anderson, C.M. & Lia, B. (1999). Infant temporal contrast sensitivity functions (tCSFs) mature earlier for luminance than for chromatic stimuli: Evidence for precocious magnocellular development? *Vision Research* **39**, 3223–3239.

Drenhaus, U., Von Gunten, A., & Rager, G. (1997). Classes of axons and their distribution in the optic nerve of the tree shrew (*Tupaia belangeri*). *Anatomical Record* **249**, 103–116.

Enroth-Cugell, C. & Robson, J.G. (1966). The contrast sensitivity of retinal ganglion cells of the cat. *Journal of Physiology* **187**, 517–552.

Freed, M.A. (2000). Parallel cone bipolar pathways to a ganglion cell use different rates and amplitudes of quantal excitation. *Journal of Neuroscience* **20**, 3956–3963.

Freed, M.A. & Sterling, P. (1988). The ON-alpha ganglion cell of the cat retina and its presynaptic cell types. *Journal of Neuroscience* **8**, 2303–2320.

Frishman, L.J., Freeman, A.W., Troy, J.B., Schweitzer-Tong, D.E. & Enroth-Cugell, C. (1987). Spatiotemporal frequency responses of cat retinal ganglion cells. *Journal of General Physiology* **89**, 599–628.

Hartveit, E. & Heggelund, P. (1993). Brain-stem influence on visual response of lagged and nonlagged cells in the cat lateral geniculate nucleus. *Visual Neuroscience* **10**, 325–339.

Hawken, M.J., Shapley, R.M. & Grosof, D.H. (1996). Temporal-frequency selectivity in monkey visual cortex. *Visual Neuroscience* **13**, 477–492.

Hochstein, S. & Shapley, R.M. (1976*a*). Quantitative analysis of retinal ganglion cell classifications. *Journal of Physiology* **262**, 237–264.

Hochstein, S. & Shapley, R.M. (1976*b*). Linear and nonlinear spatial subunits in Y cat retinal ganglion cells. *Journal of Physiology* **262**, 265–284.

Holdefer, R.N. & Norton, T.T. (1995). Laminar organization of receptive field properties in the dorsal lateral geniculate nucleus of the tree shrew (*Tupaiaglis belangeri*). *Journal of Comparative Neurology* **358**, 401–413.

Humphrey, A.L. & Saul, A.B. (1992). Action of brain-stem reticular afferents on lagged and nonlagged cells in the cat lateral geniculate nucleus. *Journal of Neurophysiology* **68**, 673–691.

Humphrey, A.L. & Saul, A.B. (1993). The temporal transformation of retinal signals in the lateral geniculate nucleus of the cat: Implications for cortical function. In *Thalamic Networks for Relay and Modulation,* ed. Minciacchi, D., Molinari, M., Macchi, G. & Jones, E.G., pp. 81–89. Oxford, UK: Pergamon Press.

Jacobs, G.H. & Neitz, J. (1986). Spectral mechanisms and color vision in the tree shrew (*Tupaia belangeri*). *Vision Research* **26**, 291–298.

Kaplan, E. & Benardete, E. (2001). The dynamics of primate retinal ganglion cells. *Progress in Brain Research* **134**, 17–33.

Kaplan, E. & Shapley, R. (1982). X and Y cells in the lateral geniculate nucleus of macaque monkeys. *Journal of Physiology* **330**, 125–143.

Kaplan, E. & Shapley, R. (1986). The primate retina contains two types of ganglion cells, with high and low contrast sensitivity. *Proceedings of the National Academy of Sciences of the U.S.A.* **83**, 2755–2757.

Kelly, D.H. & Park, M. (1972). Flicker. In *Handbook of Sensory Physiology, Vol. 7(4),* ed. Jameson, D. & Hurvich, L.M., pp. 273–302. Berlin: Springer.

Kremers, J., Lee, B.B., Pokorny, J. & Smith, V.C. (1991). The response of macaque retinal ganglion cells to complex temporal waveforms. In *From Pigments to Perception,* ed. Valberg, A. & Lee, B.B., pp. 173–176. New York: Plenum Press.

Kremers, J., Lee, B.B. & Kaiser, P.K. (1992). Sensitivity of macaque retinal ganglion cells and human observers to combined luminance and chromatic temporal modulation. *Journal of the Optical Society of America A—Optics Image Science and Vision* **9**, 1477–1485.

Kuffler, S. (1953). Discharge patterns and functional organization of mammalian retina. *Journal of Neurophysiology* **16**, 37–68.

Langham, N.P.E. (1982). The ecology of the common tree shrew, *Tupaia glis,* in peninsular Malasia. *Journal of Zoology* **197**, 323–344.

Lankheet, M.J.M., Molenaar, J. & van de Grind, W.A. (1989). Frequency transfer properties of the spike generating mechanism of cat retinal ganglion cells. *Vision Research* **21**, 1649–1661.

Lee, B.B., Elepfandt, A. & Virsu, V. (1981). Phase of response to moving sinusoidal gratings in cells of cat retina and lateral geniculate nucleus. *Journal of Neurophysiology* **45**, 807–817.

Lee, B.B., Martin, P.R. & Valberg, A. (1989). Amplitude and phase of response of macaque ganglion cells to flickering stimuli. *Journal of Physiology* **414**, 245–263.

Lee, B.B., Pokorny, J., Smith, V.C., Martin, P.R. & Valberg, A. (1990). Luminance and chromatic modulation sensitivity of macaque ganglion cells and human observers. *Journal of the Optical Society of America A—Optics Image Science and Vision* **7**, 2223–2236.

Lee, B.B., Martin, P.R., Valberg, A. & Kremers, J. (1993). Physiological mechanisms underlying psychophysical sensitivity to combined luminance and chromatic modulation. *Journal of the Optical Society of America A—Optics Image Science and Vision* **10**, 1403–1412.

Lee, B.B., Pokorny, J., Smith, V.C. & Kremers, J. (1994). Responses to pulses and sinusoids in macaque ganglion cells. *Vision Research* **34**, 3081–3095.

Lennie, P. (1980). Perceptual signs of parallel pathways. *Philosophical Transactions of the Royal Society B* (London) **290**, 23–27.

Lu, H. & Petry, H.M. (2001). Temporal properties of single neurons in the tree shrew visual system: Comparisons from progressive levels of visual processing. *Investigative Ophthalmology and Visual Science* **42**, S405.

Lu, S.M., Guido, W., Vaughan, J.W. & Sherman, S.M. (1995). Latency variability of responses to visual stimuli in cells of the cat's lateral geniculate nucleus. *Experimental Brain Research* **105**, 7–17.

Luckett, W.P. (1980). *Comparative Biology and Evolutionary Relationships of Tree Shrews*. New York: Plenum Press.

Mastronarde, D.N. (1987*a*). Two classes of single-input X-cells in cat lateral geniculate nucleus. I. Receptive-field properties and classification of cells. *Journal of Neurophysiology* **57**, 357–380.

Mastronarde, D.N. (1987*b*). Two classes of single-input X-cells in cat lateral geniculate nucleus. II. Retinal inputs and the generation of receptive-field properties. *Journal of Neurophysiology* **57**, 381–413.

Mastronarde, D.N., Humphrey, A.L. & Saul, A.B. (1991). Lagged Y cells in the cat lateral geniculate nucleus. *Visual Neuroscience* **7**, 191–200.

Movshon, J.A., Thompson, I.D. & Tolhurst, D.J. (1978). Spatial and temporal contrast sensitivity of neurons in area 17 and 18 of the cat's visual cortex. *Journal of Physiology* **283**, 101–120.

Müller, B. & Peichl, L. (1989). Topography of cones and rods in the tree shrew retina. *Journal of Comparative Neurology* **282**, 581–594.

Naka, K.I. & Rushton, W.A. (1966). S-potentials from colour units in the retina of fish (*Cyprinidae*). *Journal of Physiology* **185**, 536–555.

Norton, T.T. & Casagrande, V.A. (1982). Laminar organization of receptive-field properties in lateral geniculate nucleus of bush baby (*Galago crassicaudatus*). *Journal of Neurophysiology* **47**, 715–741.

Norton, T.T., Rager, G. & Kretz, R. (1985). On and Off regions in layer IV of striate cortex. *Brain Research* **327**, 319–323.

Peichl, L., Ott, H. & Boycott, B.B. (1987). Alpha ganglion cells in mammalian retinae. *Proceedings of the Royal Society B* (London) **231**, 169–197.

Perry, V.H., Oehler, R. & Cowey, A. (1984). Retinal ganglion cells that project to the dorsal lateral geniculate nucleus in the macaque monkey. *Neuroscience* **12**, 1101–1123.
Petry, H.M. & Hárosi, F.I. (1990). Visual pigments of the tree shrew (*Tupaia Belangeri*) and greater galago (*Galago crassicaudatus*): A microspectrophotometric investigation. *Vision Research* **30**, 839–851.
Petry, H.M. & Kelly, J.P. (1991). Psychophysical measurement of spectral sensitivity and color vision in red-light-reared tree shrews (*Tupaia belangeri*). *Vision Research* **31**, 1749–1757.
Petry, H.M., Fox, R. & Casagrande, V.A. (1984). Spatial contrast sensitivity of the tree shrew. *Vision Research* **24**, 1037–1042.
Polson, M.C. (1968). *Spectral sensitivity and color vision in* Tupaia glis. Doctoral Dissertation, Indiana University, Bloomington, IN.
Robinson, D.W. & Chalupa, L.M. (1997). The intrinsic temporal properties of alpha and beta retinal ganglion cell are equivalent. *Current Biology* **7**, 366–374.
Saul, A.B. & Humphrey, A.L. (1990). Spatial and temporal response properties of lagged and nonlagged cells in cat lateral geniculate nucleus. *Journal of Neurophysiology* **64**, 206–224.
Saul, A.B. & Humphrey, A.L. (1992). Temporal-frequency tuning of direction selectivity in cat visual cortex. *Visual Neuroscience* **8**, 365–372.
Schafer, D. (1969). Experiments on the physiology of the eye of the tree shrew *Tupaia glis*. *Journal of Comparative Physiology* **63**, 204–226.
Schiller, P.H. & Malpeli, J.G. (1977). Properties and tectal projections of monkey retinal ganglion cells. *Journal of Neurophysiology* **40**, 428–445.
Schiller, P.H. & Malpeli, J.G. (1978). Functional specificity of lateral geniculate nucleus laminae of the rhesus monkey. *Journal of Neurophysiology* **41**, 788–797.
Schiller, P.H., Finlay, B.L. & Volman, S.F. (1976). Quantitative studies of single-cell properties in monkey striate cortex. I. Spatiotemporal organization of receptive fields. *Journal of Neurophysiology* **39**, 1288–1319.
Sclar, G. (1987). Expression of "retinal" contrast gain control by neurons of the cat's lateral geniculate nucleus. *Experimental Brain Research* **66**, 589–596.
Shapley, R. & Perry, V.H. (1986). Cat and monkey retinal ganglion cells and their visual functional roles. *Trends in Neuroscience* **9**, 229–235.
Shapley, R.M. & Victor, J.D. (1978). The effect of contrast on the transfer properties of cat retinal ganglion cells. *Journal of Physiology* **285**, 275–298.
Shapley, R.M. & Victor, J.D. (1979). Nonlinear spatial summation and the contrast gain control of cat retinal ganglion cells. *Journal of Physiology* **290**, 141–161.
Sherman, S.M., Norton, T.T. & Casagrande, V.A. (1975). X- and Y-cells in the dorsal lateral geniculate nucleus of the tree shrew (*Tupaia glis*). *Brain Research* **93**, 152–157.
Silveira, L.C. & Perry, V.H. (1991). The topography of magnocellular projecting ganglion cells (M-ganglion cells) in the primate retina. *Neuroscience* **40**, 217–237.
Sturr, J.F. & Shansky, M.S. (1971). Cortical and subcortical responses to flicker in cats. *Experimental Neurology* **33**, 279–290.
ter Laak, H.J. & Thijssen, J.M. (1978). Receptive field properties of optic tract fibers from on-center sustained and transient cells in a tree shrew (*Tupaia chinensis*). *Vision Research* **18**, 1097–1109.
Thijssen, J.M., van Dongen, P.A.M. & ter Laak, H.J. (1976). Maintained activity of cells in the tree shrew's optic tract. *Experimental Brain Research* **25**, 279–290.
Tigges, J., Brooks, B.A. & Klee, M.R. (1967). ERG recordings of a primate pure cone retina (*Tupaia glis*). *Vision Research* **7**, 553–563.
Troy, J.B. & Shou, T. (2002). The receptive fields of cat retinal ganglion cells in physiological and pathological states: Where we are after half a century of research. *Progress in Retinal Research* **21**, 263–302.
Uhlrich, D.J., Tamamaki, N. & Sherman, M. (1990). Brainstem control of response modes in neurons of the cat's lateral geniculate nucleus. *Proceedings of the National Academy of Sciences of the U.S.A.* **87**, 2560–2563.
van Dongen, P.A.M., ter Laak, H.J., Thijssen, J.M. & Vendrik, A.J.H. (1976). Functional classification of cells in the optic tract of a tree shrew (*Tupaia chinensis*). *Experimental Brain Research* **24**, 441–446.
Victor, J.D. (1987). The dynamics of the cat retinal X-cell center. *Journal of Physiology* **386**, 219–246.
Victor, J.D. & Shapley, R.M. (1979). Receptive field mechanisms of cat X and Y retinal ganglion cells. *Journal of General Physiology* **74**, 275–298.
Watanabe, M. & Rodieck, R.W. (1989). Parasol and midget ganglion cells of the primate retina. *Journal of Comparative Neurology* **289**, 434–454.
Werblin, F.S. & Dowling, J.E. (1969). Organization of the retina of the mudpuppy, *Necturus maculosus*. II. Intracellular recording. *Journal of Neurophysiology* **32**, 339–355.
Wilson, H.R. (1978). Quantitative prediction of line spread function measurements: Implications for channel bandwidths. *Vision Research* **18**, 493–496.
Wolfe, J.M. & Palmer, L.A. (1998). Temporal diversity in the lateral geniculate nucleus of cat. *Visual Neuroscience* **15**, 653–675.
Yeh, T., Lee, B.B., Kremers, J., Cowing, J.A., Hunt, D.M., Martin, P.R. & Troy, J.B. (1995). Visual responses in the lateral geniculate nucleus of dichromatic and trichromatic marmosets (*Callithrix jacchus*). *Journal of Neuroscience* **15**, 7892–7904.